**Title: A remotely sensed pigment index reveals photosynthetic phenology in evergreen conifers**

**Authors**: John A. Gamon[1,2], K. Fred Huemmrich[3], Christopher Y.S. Wong[4,5], Ingo Ensminger[4,5,6], Steven Garrity[7], David Y. Hollinger[8], Asko Noormets[9], Josep Peñuelas[10,11]

[1]CALMIT (Center for Advanced Land Management Information Technologies), School of Natural Resources, University of Nebraska – Lincoln, 307 Hardin Hall, 3310 Holdrege St., Lincoln, NE, 68583-0989 USA
[2]Departments of Earth and Atmospheric Sciences & Biological Sciences, University of Alberta, Edmonton, AB, Canada
[3]University of Maryland Baltimore County, Code 618, NASA's Goddard Space Flight Center, Greenbelt, MD 20771
[4]Department of Biology, University of Toronto, 3359 Mississauga Road, Mississauga, L5L1C6 ON, Canada
[5]Graduate Department of Ecology and Evolutionary Biology, University of Toronto, Toronto M5S 1A1, ON, Canada
[6]Graduate Department of Cell and Systems Biology, University of Toronto, Toronto M5S 3G5, ON, Canada
[7]Steven R. Garrity, Decagon Devices, Inc., 2365 NE Hopkins Ct., Pullman, WA 99163, USA.
[8]US Forest Service, Northern Research Station, 271 Mast Rd. Durham, NH 03824, USA
[9]Dept. Forestry and Environmental Resources, North Carolina State University, 920 Main Campus Drive, Suite 300, Raleigh NC 27695, USA.
[10]CSIC, Global Ecology Unit CREAF-CEAB-CSIC-UAB, Bellaterra 08193, Catalonia, Spain
[11]CREAF, Center for Ecological Research and Forestry Applications, Cerdanyola del Vallès, 08193, Catalonia, Spain.

**Abstract**
In evergreen conifers, where the foliage amount changes little with season, accurate detection of the underlying "photosynthetic phenology" from satellite remote sensing has been difficult, presenting challenges for global models of ecosystem carbon uptake. Here, we report a close correspondence between seasonally changing foliar pigment levels, expressed as chlorophyll/carotenoid ratios, and evergreen photosynthetic activity, leading to a "chlorophyll/carotenoid index" (CCI) that tracks evergreen photosynthesis at multiple spatial scales. When calculated from NASA's Moderate Resolution Imaging Spectroradiometer satellite sensor, the CCI closely follows the seasonal patterns of daily gross primary productivity of evergreen conifer stands measured by eddy covariance. This discovery provides a way of monitoring evergreen photosynthetic activity from optical remote sensing, and indicates an important regulatory role for carotenoid pigments in evergreen photosynthesis. Improved methods of monitoring photosynthesis from space can improve our understanding of the global carbon budget in a warming world of changing vegetation phenology.

Keywords: carotenoid pigments, evergreen conifers, gross primary productivity (GPP), Chlorophyll:Carotenoid Index (CCI)

**Significance Statement**

Evergreen photosynthetic activity has been difficult to determine from remote sensing, causing errors in terrestrial photosynthetic carbon uptake models. Using a reflectance index (CCI) sensitive to seasonally changing chlorophyll:carotenoid pigment ratios, we demonstrate a method of tracking photosynthetic phenology in evergreen conifers. CCI reveals seasonally changing photosynthetic rates and detects the onset of the growing season in evergreen foliage. This method could improve our understanding of changing photosynthetic activity in a warming climate, and could improve assessment of the evergreen component of the terrestrial carbon budget, which has been elusive.

**Significance**
Evergreen photosynthetic activity has been difficult to determine from remote sensing, causing errors in terrestrial photosynthetic carbon uptake models. Using a reflectance chlorophyll/carotenoid index (CCI) sensitive to seasonally changing chlorophyll/carotenoid pigment ratios, we demonstrate a method of tracking photosynthetic phenology in evergreen conifers. The CCI reveals seasonally changing photosynthetic rates and detects the onset of the growing season in evergreen foliage. This method could improve our understanding of changing photosynthetic activity in a warming climate, and could improve assessment of the evergreen component of the terrestrial carbon budget, which has been elusive.

**/body**

## Introduction

The biosphere helps regulate atmospheric composition and climate, in part through the exchange of radiatively active gases, primarily carbon dioxide. About half of the "extra" carbon added to the atmosphere by human activity is rapidly absorbed by the biosphere, effectively slowing climate change relative to what would occur without this uptake (1, 2). The exact mechanism and spatiotemporal distribution of the terrestrial component of this carbon sink have been ongoing research topics for many years. In a warming world, the timing of photosynthetic activity is also changing, with unknown impacts on ecosystem productivity. These shifting patterns of seasonal photosynthetic activity, or "photosynthetic phenology," affect the biospheric-atmospheric gas exchange, further influencing atmospheric composition and climate (3–5). Faced with these uncertainties, quantifying the spatial and temporal patterns of biosphere/atmosphere carbon fluxes for different biomes and understanding their proximal controls remain central goals of global carbon cycle science.

Northern forests make a large contribution to global photosynthetic carbon fixation and are an important component of the global carbon budget. However, northern evergreen conifers, including evergreen conifers of the vast boreal regions, present particular challenges to global carbon cycle monitoring (6). Their seasonal activity may be changing with an earlier growing season, with important implications for the biospheric carbon budget. A simple hypothesis has been that a longer growing season results in greater carbon uptake, particularly for northern ecosystems where photosynthetic activity has been temperature-limited (3, 7). By contrast, warmer growing seasons are also more likely to cause drought, restricting ecosystem carbon uptake and enhancing ecosystem respiration, resulting in accelerated carbon losses to the atmosphere (8). The actual outcome of changing seasonality on the biospheric carbon budget remains an open question, with multiple factors likely to be important.

A primary tool for assessing terrestrial carbon uptake has been eddy covariance, which provides near-direct assessment of surface/atmosphere carbon fluxes. Although it provides an excellent means of sampling the gas exchange of representative ecosystems for limited regions (9), it must be supplemented by other less costly and more spatially extensive methods for global carbon flux assessments. Remote sensing provides an ideal means of extrapolating flux measurements beyond the sampling footprint of individual flux towers to larger regions. Accurate methods of tracking photosynthetic phenology using remote sensing are critical to a full understanding of the impact of climate variation on terrestrial gross primary productivity (GPP) and to a proper assessment of the global carbon budget. With global, daily satellite coverage, we now have the means of generating wall-to-wall images of photosynthetic carbon uptake and net primary productivity for virtually the entire planet. For example, the MOD17 algorithm based on the light-use efficiency (LUE) model (10) states that daily GPP, or gross primary production, is a product of absorbed radiation (APAR) and the efficiency («) with which this absorbed energy is converted to fixed carbon:

$$GPP = APAR \times \varepsilon \quad (1)$$

*APAR*, in turn, is a product of irradiance in the photosynthetically active radiation (PAR) region of the spectrum (i.e., 400–700 nm) and the *fraction* of that PAR irradiance that is absorbed by green vegetation ($f_{APAR}$):

$$APAR = f_{APAR} \times PAR \quad (2)$$

The $f_{APAR}$ term is closely related to the normalized difference vegetation index (NDVI), a measure of vegetation greenness, and the PAR term is typically obtained from meteorological data (10, 11).

For much of the world's deciduous or annual vegetation, where the seasonal expression of photosynthetic activity closely follows green canopy display, the APAR term largely captures the seasonal photosynthetic dynamics (11). However, evergreen vegetation poses particular challenges for the LUE model. For evergreens that retain their foliage through the seasons, the *f*PAR component of the APAR term is relatively stable compared with *f*PAR for annual or deciduous vegetation, providing insufficient
information on the actual seasonal dynamics of photosynthetic activity. Assessing « has been more challenging than measuring APAR from remote sensing, in part because « is highly variable in time and space (12). Particularly for northern evergreen conifers that experience periods of photosynthetic down-regulation during winter dormancy or chronic stress, « emerges as an important determinant of seasonal photosynthetic activity (13). Conventional vegetation indices (e.g., NDVI) that are responsive to changes in green leaf area typically fail to detect these seasonal photosynthetic dynamics (12, 14), leading to errors in satellitedriven ecosystem productivity models. Not surprisingly, although the MOD17 algorithm depicts broad-scale seasonal dynamics of photosynthetic activity for different biomes, it sometimes fails to reproduce faithfully annual sums or seasonal patterns of ecosystem photosynthetic activity measured by flux towers (15), and
it does not capture local heterogeneity in $\varepsilon$[16].

Due to these challenges, many studies have sought to improve the LUE model by assessing « directly from remote sensing (12). One approach involves remote detection of the xanthophyll cycle, which adjusts the distribution of absorbed light energy through the interconversion of a group of three carotenoid pigments (17). This biochemical response can be detected with proximal remote sensing using the photochemical reflectance index (PRI), which provides a direct method of assessing changing LUE over short time spans (18–20). However, over annual time periods, the primary driver of the PRI at leaf and canopy scales is the changing leaf carotenoid pigment pool, typically expressed as the changing ratio of chlorophyll to carotenoid pigments (or its inverse), and not the xanthophyll cycle *per se* (21–25). This observation of changing pigment content is particularly relevant for northern evergreen conifers that undergo large seasonal swings in photosynthetic activity and carotenoid pigment levels associated with temperature extremes (24–28). These findings have led us to reconsider the function of carotenoid pigments in the context of detecting photosynthetic phenology in evergreen conifers.

Carotenoids serve many important roles in plants. They function as light capture and photoprotective pigments; act as antioxidants; and are linked to the synthesis of isoprenoids, which are produced under high-temperature stress (29). Carotenoid levels increase when plants are exposed to a variety of environmental stressors. This finding leads to the hypothesis that enhanced carotenoid levels, typically expressed relative to chlorophyll content, provide optical indicators of reduced photosynthetic activity and LUE. A large body of literature indicates that chlorophyll/carotenoid ratios decrease in evergreen leaves during winter cold (27, 30–32). Field studies have confirmed that chlorophyll/ carotenoid ratios closely track the seasonal photosynthetic activity of Mediterranean climate evergreen leaves (21, 23). This conclusion is further supported by recent spectral and kinetic evidence that demonstrates a close coincidence between seasonal photosynthetic activity, chlorophyll/carotenoid ratios, and spectral reflectance in evergreen conifers (24–26). Together, these studies suggest that satellite indices of changing pigment levels might provide reliable indicators of evergreen photosynthetic phenology.

In this study, we consider whether newly available combinations of satellite bands from NASA's Moderate Resolution Imaging Spectroradiometer (MODIS) sensors can provide useful metrics of seasonal changing pigment levels and photosynthetic activity in evergreen conifers. Our analysis was made possible by the recent reprocessing of MODIS data (MODIS collection 6) that provides both ocean and land band surface reflectance products over terrestrial areas, affording new options for assessing evergreen photosynthetic activity. Because the original PRI bands (33, 34) are not available from the MODIS, we considered new band combinations (MODIS bands 1 and 11) indicative of chlorophyll/carotenoid ratios, and used leaf- and stand-level experiments to confirm the interpretation of these bands independently.

**Results**

In conifers, reflectance from evergreen leaves exhibits distinct seasonal changes, particularly in the green-red spectral region (550–650 nm) (Fig. 1). The wintertime increase in reflectance at these wavelengths indicates a decreased chlorophyll/carotenoid pigment ratio, often visible to a careful observer as a wintertime needle yellowing. MODIS bands 11 (531 nm) and 1 (645 nm) captured the contrasting behavior of evergreen leaf reflectance in these two spectral regions (Fig. 1). MODIS band 1 (645 nm, a terrestrial band) is clearly affected by the increased red reflectance, whereas band 11 (531 nm, an ocean band) changes little or undergoes a slight decline in reflectance during winter.

Parallel to the seasonal leaf reflectance changes (Fig. 1), the leaves exhibited substantial photosynthetic down-regulation during winter, detectable as changes in reflectance, pigment levels, and photosynthetic rates (Fig. 2). Leaf chlorophyll/carotenoid ratios declined gradually in fall and winter, and then recovered rapidly in spring (Fig. 2). Photosynthetic rates exhibited a similar rapid spring increase (Fig. 2). The chlorophyll/carotenoid index (CCI) responded near synchronously to these seasonal changes in pigment ratios and photosynthetic activity, both at the leaf and stand level (Fig. 2).

We then examined the CCI generated from satellite-derived surface reflectance for several evergreen-dominated North American flux tower sites (Table S1) using the newly available

MODIS collection 6. As with the leaf- and stand-scale measurements of evergreen seedlings (Fig. 2), the CCI closely tracked the seasonal dynamics of photosynthesis, expressed as daily GPP at each site in this case (Fig. 3). In contrast, the NDVI showed a weaker seasonal response that was out of phase with photosynthetic activity, lagging GPP and CCI in fall and winter. Further analysis (Fig. S1 and Table S2) showed that the MODIS CCI index was significantly correlated with daily GPP for each site and for all sites combined, with noticeable variation in the CCI-GPP patterns between stands. Not surprisingly, the commonly used NDVI greenness index was a weaker predictor of daily GPP (Table S2), illustrating the limitation of conventional vegetation greenness indices for assessing the invisible photosynthetic phenology of evergreens. This limitation was particularly clear for the Wind River site, where the NDVI showed relatively little sensitivity to seasonally changing GPP. For each of the other two sites (North Carolina and Howland, Maine), both of which had larger contributions to the optical signals from deciduous species (Table S1), there was a stronger seasonal NDVI response than for the Wind River stand, which had a predominantly evergreen overstory.

**Discussion**

These results illustrate the possibility of a pigment-based index (CCI) for monitoring the terrestrial biosphere. The CCI provides a metric of photosynthetic phenology in evergreens that can be applied at both leaf and stand levels. The close correspondence between the CCI and photosynthetic activity at the leaf scale (Fig. 2), and GPP at the ecosystem scale for a variety of evergreen stands (Fig. 3), demonstrates the promise of pigment-based approaches to remote monitoring of evergreen photosynthetic activity.

The seasonal behavior of carotenoid pigment pools is consistent with a body of literature indicating an important role for carotenoid pigments in wintertime down-regulation and photoprotection. A wintertime photoprotective function for xanthophyll cycle pigments is well-established (27, 30–32). However, we note that a variety of carotenoids, particularly lutein and, to a lesser extent, beta-carotene, as well as xanthophyll cycle pigments, contributed to the large pigment pool size shift that coincided with the seasonally changing CCI index and photosynthetic activity (Fig. S2). These observations demonstrate that the changes in seasonal pigment levels involve additional pigments and photoprotective mechanisms besides the xanthophyll cycle, and are consistent with reports of a similar photoprotective role for lutein (35).

The PRI, which uses a band (531 nm) close to MODIS band 11, but a different reference band (570 nm), similarly tracks seasonally changing pigment ratios and photosynthetic rate (21, 23–26). Because the exact PRI bands are not available from MODIS, several studies have considered indices derived from MODIS bands similar to the PRI bands, often by combining MODIS band 11 with an alternate reference band. Some of these studies have compared the same MODIS bands reported here with seasonal change in photosynthesis for evergreen forests, with promising results (36, 37). Although these new satellite band combinations have sometimes been called “MODIS PRI” bands, we note that they are spectrally and functionally different from the original PRI bands used to characterize the diurnal xanthophyll cycle response. Unlike the PRI, which was designed to track shortterm reflectance changes at 531 nm, these MODIS bands are primarily responding to changing

red reflectance (Fig. 1) due to changing pigment pools (Fig. 2), and actually indicate shifting chlorophyll and carotenoid pigment levels rather than the xanthophyll cycle per se, particularly when sampled over seasonal cycles (24–26, 28). Given the link to chlorophyll and carotenoid pigments (Fig. 2), the different bands used, and the seasonal (rather than diurnal) variation in leaf pigment pools involved, the CCI reflects these actual pigment changes and is distinct from the PRI, which was originally derived to monitor xanthophyll cycle activity and LUE over diurnal time scales (18, 33).

In our study, we chose to use MODIS because it provides data products at spatial and temporal scales suitable for comparison with eddy covariance data. The advent of MODIS collection 6 now provides a standardized surface reflectance product, including land and ocean bands. Consequently, a global CCI is now becoming widely available, and offers a practical means of assessing pigment dynamics associated with seasonal changes in photosynthetic activity in evergreens, where established greenness indices (e.g., NDVI, *f*PAR, leaf area index) cannot properly capture this seasonal photosynthetic activity. Of particular significance is the similar behavior of the CCI across three evergreen conifer stands and several spatial scales, including ground sampling at leaf and stand scales and whole-ecosystem satellite measurements. This scale independence suggests that the CCI can provide a potent metric of evergreen photosynthetic phenology from a variety of remote sensing platforms, and can be supported by ground sampling that assesses pigment levels or foliage optical properties.

Although we describe these stands as predominantly "evergreen" conifer stands, they actually included varying deciduous components that likely contributed to variation in CCI and NDVI responses across stands (Table S1). This varying stand composition and levels of deciduousness helps explain the contrasting seasonal CCI and NDVI patterns for these sites (Fig. 3). These possibilities can be further investigated by independent ground studies characterizing physiological responses (as shown in Figs. 1 and 2), stand composition, and latitudinal (including angular) effects on the optical signals. Currently, there is a growing network of ground optical validation sites located at flux towers (38–40), and these sites can be equipped to test the relative merits of the NDVI, PRI, and CCI further for monitoring ecosystem photosynthesis. Such independent ground validation is needed because any two-band index can be affected by multiple factors, often causing misinterpretation of underlying biophysical traits or processes when satellite data are used alone. To clarify the contribution of these multiple factors, we propose that extended ground sampling networks using flux tower sites be used in future studies of changing photosynthesis and productivity from global satellite sensors. Despite these remaining questions, the strongly similar seasonal responses across the three sites and across spatial scales shown here, along with similar findings from Mediterranean evergreen vegetation (36), suggest that the CCI offers a widely applicable indicator of photosynthetic activity and GPP for evergreen-dominated ecosystems. We note, however, that our study does not consider all evergreen-dominated biomes (e.g., tropical moist broadleaved forests, where satellite and flux data observations are more limited).

More work is now needed to reconsider the parameterization of the LUE model in light of these findings, which could help develop new upscaling approaches. A current working hypothesis is that the NDVI, PRI, and CCI provide complementary information about

photosynthetic phenology. The NDVI closely follows seasonal photosynthetic activity related to green leaf display in annual and deciduous vegetation, whereas the CCI and PRI add additional information about photosynthetic regulatory processes involving photoprotective pigments and appear to be particularly useful in evergreens (28). Like the CCI, the PRI responds to seasonal pigment shifts associated with photosynthetic downregulation in evergreens (24, 25), but it is also sensitive to short periods of down-regulation mediated by the xanthophyll cycle (e.g., midday photosynthetic depression due to summer drought) (41). In the future, LUE model parameterizations should explicitly recognize that these two indices reveal contrasting effects on photosynthetic activity over different time scales (28).

Recently, a similar ability to track photosynthetic phenology from satellites has been reported using solar-induced fluorescence (SIF), which provides an alternate method of assessing photosynthetic activity from remote sensing (6, 42). Because the CCI index is based on reflectance, which has a well-established methodology and history, it can provide a strong foundation for interpreting the *causes* of changes in SIF. However, SIF is not currently available at a temporal or spatial scale comparable to the MODIS, making a direct comparison with a MODIS-derived CCI difficult without considerable data aggregation and associated loss of spatial or temporal resolution that would conceal the underlying mechanisms addressed here. Combined measurement of SIF and pigment indices has been proposed recently as part of the FLuorescence EXplorer (FLEX) satellite mission (43), and could lead to an improved assessment of photosynthetic phenology, particularly for evergreens that have been difficult to measure from satellites using more conventional vegetation indices (e.g., the NDVI). To fully understand the significance of plant pigments as functional indicators, a full spectral ("hyperspectral") satellite imaging spectrometer would be ideal. Such sensors are available on airborne platforms (44) and as demonstration satellite missions (45), none of which provide frequent global coverage; and thus cannot properly assess diurnal or seasonal photosynthetic dynamics for large regions of the planet. Proposed satellite-based imaging spectrometers (43, 46) could further our understanding of these functionally different pigment responses for different ecosystems, opening further unseen possibilities for monitoring photosynthesis from space.

This study extends our previous understanding of carotenoid pigments by relating their seasonal patterns to the seasonal patterns of reflectance and photosynthesis in evergreen conifers. The CCI derived from a new combination of MODIS bands 1 and 11 offers a promising tool for observing photosynthetic phenology of terrestrial ecosystems. If properly coupled with field validation, such measurements could greatly improve our understanding of the changing photosynthetic phenology of evergreen stands that have been difficult to assess with conventional satellite indices. Assessment of evergreen pigment activity can improve our ability to measure carbon cycle dynamics for this important component of the world's vegetation.

## Methods

**Sites and Plant Materials.** Leaf- and stand-scale measurements were conducted on potted 4-y-old lodgepole pine (*Pinus contorta*) seedlings grown outdoors under ambient

conditions in full sun at the University of Alberta campus (Edmonton, Alberta, Canada; 53.5289°N, 113.5261°W). Plants were arranged in closed-canopy stands. Initially planted in 2010 in 2.3-L pots, they were repotted in subsequent years into 2.8-L and 6.2-L pots in a 1:2 soil mixture of sandy top soil and potting soil (Sunshine Mix 4; Sun Gro Horticulture). The seedlings were irrigated throughout the growing season to avoid drought stress. Stand-scale eddy covariance measurements (described below) were obtained from sites spanning a wide range of species, edaphic, climatic, geographic location, and canopy structural conditions (Table S1).

**Leaf Pigment Measurements.** Leaves were collected immediately after leaf reflectance measurements from the same six trees sampled every 1–2 wk. The sampled leaves were frozen in liquid nitrogen and later transferred into a−80 °C freezer for long-term storage. For each sampling date, six 1-cm-long segments from each seedling were pooled together for pigment analysis using HPLC (1260 Infinity; Agilent Technologies) following the method of Thayer and Björkman (47) to determine carotenoid and chlorophyll pigment quantities. Commercial pigment standards (DHI LAB Products) were used to calibrate the HPLC system for pigment quantification. Chlorophyll/carotenoid pigment ratios were determined from total chlorophyll (a and b) and total carotenoids (neoxanthin, violaxanthin, antheraxanthin, zeaxanthin, lutein, and β -carotene concentrations).

**Leaf Gas Exchange Measurements.** Foliar gas exchange was measured using a portable photosynthesis system (LI-6400; LI-COR). Each measurement consisted of a light-response curve ranging from 0 to 1,500 μmol·m−2·s−1. Measurements were taken at each light level when steady-state photosynthesis was obtained, typically within 3 min. The chamber CO2 concentration was set to 395 μmol·m−2·s−1, and temperature was set to match ambient conditions. Photosynthetic rate was expressed as light-saturated photosynthesis, which was estimated from the saturation point of the light response curves. The same six plants from the reflectance measurements were monitored on a weekly basis during spring recovery of photosynthetic activity.

**Flux Data.** Daily GPP values were retrieved from the FLUXNET "LaThuile" dataset (www.fluxdata.org/default.aspx) for three sites (Table S1). These values were calculated from eddy covariance measurements that were filtered, despiked, and gap-filled, and the net ecosystem exchange was partitioned into daily GPP and ecosystem respiration following standard algorithms (48, 49).

**Leaf Spectral Measurement.** Leaf-scale reflectance was measured with a portable spectrometer (UniSpec SC; PP Systems) equipped with a bifurcated fiber optic (UNI410; PP Systems) and needle leaf clip (UNI501; PP Systems). Leaves of six plants (five randomly selected, sunlit leaves per plant) were monitored through the course of the study. Leaves were sampled at around 1300 hours under sunlight every 1–2 wk. Each set of leaf measurements for a given plant consisted of an average of 10 samples and was preceded by a dark scan and a reference scan from a Spectralon white standard (Labsphere) to obtain reflectance values.

**Whole-Stand Spectral Measurements.** Reflectance was also measured on experimental stands of the same seedlings used for leaf reflectance with a portable spectrometer (UniSpec-DC; PP Systems). An upward-facing fiber (UNI686; PP Systems) attached to a

cosine receptor (UNI435; PP Systems) measured incoming irradiance. A downward-facing fiber (UNI684; PP Systems) fitted with a field-of-view (FOV) restrictor (UNI688; PP Systems) limited the FOV to 15° for measuring stand radiance. For each measurement date, 12 measurements were taken from a position ~0.5 m above the canopy, each covering a different location of the stand at around 1330 hours every week during spring recovery. Each set of canopy measurements was preceded by a dark scan and a reference scan from a white standard panel (Spectralon; Labsphere) to obtain reflectance values.

**MODIS Satellite Data.** Optical data from MODIS onboard the Aqua satellite were processed to surface reflectance using the multi-angle implementation of atmospheric correction (MAIAC) algorithm (50, 51). The MAIAC algorithm makes use of time-series and spatial analyses for cloud screening and aerosol retrievals (52, 53). MAIAC terrestrial surface reflectances were gridded at a resolution of 1 km, and both MODIS land and ocean bands were processed (MODIS bands 1–12), providing reflectance in spectral bands that have previously been used on a limited basis for terrestrial applications (16, 37, 54). In this analysis, a time series of surface reflectance values was extracted for the 1-km grid that included the location of the flux tower. All cloud-free observations with high data quality and view zenith angles less than 45° were used.

**CCI Calculations.** From the MODIS satellite sensor, the CCI was calculated from reflectance using MODIS bands 1 and 11 reflectance ($\rho$) as $(\rho_{B11}- \rho_{B1})/( \rho_{B11}+ \rho_{B1})$. From leaf- and stand-level reflectance, the reflectance spectra were first interpolated to 1-nm intervals. MODIS band reflectance values were then simulated by convolving the 1-nm reflectance values against the MODIS bandpass responses for bands 1 and 11. The CCI was then calculated using the simulated MODIS bands 1 and 11, respectively.

**Statistical Analysis.** Regression statistics and analyses of covariance were conducted in R (R Studio).

**Acknowledgements:**
We thank Dave Landis (GST, Inc.) for MODIS data processing. J.A.G. was supported by the Alberta Informatics Circle of Research Excellence/Alberta Innovates Technology Futures (Grants G224150012 and 200700172), Natural Sciences and Engineering Research Council (NSERC) (Grant RGPIN-2015-05129), Canada Foundation for Innovation (CFI) (Grant 26793), and NASA Arctic-Boreal Vulnerability Experiment (Grant NNX15AT78A). K.F.H. was supported by the NASA Science of Aqua and Terra program (Grant NNX14AJ65G). I.E. was supported by the NSERC (Grant RGPIN-2015-06514), CFI (Grant 27330), and Ontario Ministry of Research and Innovation (Grant ER10- 07-015). J.P. was supported by European Research Council Synergy Grant SyG-2013-610028 IMBALANCE-P. Data and logistical support for theWind River site were provided by the US Forest Service (FS) Pacific Northwest Research Station and the University ofWashington (Grant 11-JV-11261952-030). Support for the Howland Forest AmeriFlux core site was provided by the US Department of Energy (DOE)'s Office of Science and the US Department of Agriculture (USDA) Forest Service Northern Research Station. The work at the Parker Tract, NC (USNC2) site was supported by USDA FS Eastern Forest Environmental Threat Assessment Center Cooperative Agreements 03-CA-11330147-073 and 04-CA-11330147-238, DOE-National Institute

for Climate Change Research (NICCR) Award 08-SC-NICCR-1072, Department of the Interior (DOI) Southeast Climate Science Center Award G10AC00624, DOE Terrestrial Ecosystem Science Award 11-DE-SC-0006700, and USDA NIFA Awards 2011-68002-30185 and 2014-67003-22068.

**References**

1. Canadell JG, et al. (2007) Contributions to accelerating atmospheric CO2 growth from economic activity, carbon intensity, and efficiency of natural sinks. Proc Natl Acad Sci USA 104(47):18866–18870.
2. Raupach MR, et al. (2014) The declining uptake rate of atmospheric CO2 by land and ocean sinks. Biogeosciences 11:3453–3475.
3. Randerson JT, Field CB, Fung IY, Tans PP (1999) Increases in early season ecosystem uptake explain recent changes in the seasonal cycle of atmospheric CO2 at high northern latitudes. Geophys Res Lett 26:2765–2768.
4. Peñuelas J, Rutishauser T, Filella I (2009) Ecology. Phenology feedbacks on climate change. Science 324(5929):887–888.
5. Richardson AD, et al. (2013) Climate change, phenology, and phenological control of vegetation feedbacks to the climate system. Agriculture and Forest Meteorology 169:156–173.
6. Walther S, et al. (2016) Satellite chlorophyll fluorescence measurements reveal largescale decoupling of photosynthesis and greenness dynamics in boreal evergreen forests. Glob Change Biol 22(9):2979–2996.
7. Myneni RB, Keeling CD, Tucker CJ, Asrar G, Nemani RR (1997) Increased plant growth in the northern high latitudes from 1981 to 1991. Nature 386:698–702.
8. Trahan MW, Schubert BA (2016) Temperature-induced water stress in high-latitude forests in response to natural and anthropogenic warming. Glob Change Biol 22(2): 782–791.
9. Baldocchi DD, Hicks BB, Meyers TP (1988) Measuring biosphere-atmosphere exchanges of biologically related gases with micrometeorological methods. Ecology 69:1331–1340.
10. Heinsch FA, et al. (2006) Evaluation of remote sensing based terrestrial productivity from MODIS using regional tower eddy flux network observations. IEEE Trans Geosci Remote Sens 44:1908–1925.
11. Running SW, et al. (2004) A continuous satellite-derived measure of global terrestrial primary production. Bioscience 54:547–560.
12. GarbulskyMF, et al. (2010) Patterns and controls of the variability of radiation use efficiency and primary productivity across terrestrial ecosystems. Glob Ecol Biogeogr 19:253–267.
13. Garbulsky MF, Peñuelas J, Gamon J, Inoue Y, Filella I (2011) The photochemical reflectance index (PRI) and the remote sensing of leaf, canopy and ecosystem radiation use efficiencies: A review and meta-analysis. Remote Sens Environ 115:281–297.
14. Gamon JA, et al. (1995) Relationships between NDVI, canopy structure, and photosynthesis in three Californian vegetation types. Ecol Appl 5:28–41.
15. Turner DP, et al. (2005) Site-level evaluation of satellite-based global terrestrial gross primary production and net primary production monitoring. Glob Change Biol 11:666–684.

16. Drolet GG, et al. (2008) Regional mapping of gross light-use efficiency using MODIS spectral indices. Remote Sens Environ 112:3064–3078.
17. Demmig-Adams B, Adams WW (1996) Chlorophyll and carotenoid composition in leaves of Euonymus kiautschovicus acclimated to different degrees of light stress in the field. Aust J Plant Physiol 23:649–659.
18. Gamon JA, Peñuelas J, Field CB (1992) A narrow-waveband spectral index that tracks diurnal changes in photosynthetic efficiency. Remote Sens Environ 41:35–44.
19. Gamon JA, Serrano L, Surfus JS (1997) The photochemical reflectance index: An optical indicator of photosynthetic radiation use efficiency across species, functional types, and nutrient levels. Oecologia 112:492–501.
20. Peñuelas J, Garbulsky MF, Filella I (2011) Photochemical reflectance index (PRI) and remote sensing of plant $CO_2$ uptake. New Phytol 191(3):596–599.
21. Stylinski CD, Gamon JA, Oechel WC (2002) Seasonal patterns of reflectance indices, carotenoid pigments and photosynthesis of evergreen chaparral species. Oecologia 131:366–374.
22. Nakaji T, Oguma H, Fujinuma Y (2006) Seasonal changes in the relationship between photochemical reflectance index and photosynthetic light use efficiency of Japanese larch needles. Int J Remote Sens 27:493–509.
23. Filella I, et al. (2009) PRI assessment of long-term changes in carotenoids/chlorophyll ratio and short-term changes in de-epoxidation state of the xanthophyll cycle. Int J Remote Sens 30:4443–4455.
24. Wong CYS, Gamon JA (2015) The photochemical reflectance index provides an optical indicator of spring photosynthetic activation in evergreen conifers. New Phytol 206(1):196–208.
25. Wong CYS, Gamon JA (2015) Three causes of variation in the photochemical reflectance index (PRI) in evergreen conifers. New Phytol 206(1):187–195.
26. Fréchette E, Wong CYS, Junker LV, Chang CY-Y, Ensminger I (2015) Zeaxanthinindependent energy quenching and alternative electron sinks cause a decoupling of the relationship between the photochemical reflectance index (PRI) and photosynthesis in an evergreen conifer during spring. J Exp Bot 66(22):7309–7323.
27. Ensminger I, et al. (2004) Intermittent low temperatures constrain spring recovery of photosynthesis in boreal Scots pine forests. Glob Change Biol 10:995–1008.
28. Gamon JA (2015) Reviews and syntheses: Optical sampling of the flux tower footprint. Biogeosciences 12:4509–4523.
29. Peñuelas J, et al. (2013) Photochemical reflectance index as an indirect estimator of foliar isoprenoid emissions at the ecosystem level. Nat Commun 4:2604.
30. Adams WW, III, Demmig-Adams B (1994) Carotenoid composition and down regulation of photosystem II in three conifer species during the winter. Physiol Plant 92:451–458.
31. Ottander C, Campbell D, Oquist G (1995) Seasonal changes in photosystem II organization and pigment composition in Pinus sylvestris. Planta 197:176–183.
32. Oquist G, Huner NPA (2003) Photosynthesis of overwintering evergreen plants. Annu Rev Plant Biol 54:329–355.
33. Gamon JA, Filella I, Peñuelas J (1993) The dynamic 531-nanometer Δ reflectance signal: A survey of twenty angiosperm species. Photosynthetic Responses to the

Environment, eds Yamamoto HY, Smith CM (American Society of Plant Physiologists, Rockville, MD), pp 172–177.
34. Peñuelas J, Filella I, Gamon JA (1995) Assessment of photosynthetic radiation-use efficiency with spectral reflectance. New Phytol 131:291–296.
35. Jahns P, Holzwarth AR (2012) The role of the xanthophyll cycle and of lutein in photoprotection of photosystem II. Biochim Biophys Acta 1817(1):182–193.
36. Garbulsky MF, Peñuelas J, Ogaya R, Filella I (2013) Leaf and stand-level carbon uptake of a Mediterranean forest estimated using the satellite-derived reflectance indices EVI and PRI. Int J Remote Sens 34:1282–1296.
37. Goerner A, Reichstein M, Rambal S (2009) Tracking seasonal drought effects on ecosystem light use efficiency with satellite-based PRI in a Mediterranean forest. Remote Sens Environ 113:1101–1111.
38. Gamon JA, Rahman AF, Dungan JL, SchildhauerM, Huemmrich KF (2006) Spectral Network (SpecNet)—What is it and why do we need it? Remote Sens Environ 103:227–235.
39. Gamon JA, et al. (2010) SpecNet revisited: Bridging flux and remote sensing communities. Can J Remote Sens 36:S376–S390.
40. Porcar-Castell A, et al. (2015) EUROSPEC: At the interface between remote-sensing and ecosystem CO2 flux measurements in Europe. Biogeosciences 12:6103–6124.
41. Ripullone F, et al. (2011) Effectiveness of the photochemical reflectance index to track photosynthetic activity over a range of forest tree species and plant water statuses. Funct Plant Biol 38:177–186.
42. Joiner J, et al. (2014) The seasonal cycle of satellite chlorophyll fluorescence observations and its relationship to vegetation phenology and ecosystem atmosphere carbon exchange. Remote Sens Environ 152:375–391.
43. Kraft S, et al. (2013) FLORIS: Phase A status of the Fluorescence Imaging Spectrometer of the Earth Explorer mission candidate FLEX. Proc SPIE 8889(88890T):1–12.
44. Green RO, et al. (1998) Imaging spectroscopy and the Airborne Visible Infrared Imaging Spectrometer (AVIRIS). Remote Sens Environ 65:227–248.
45. Middleton EM, et al. (2013) The Earth Observing One (EO-1) satellite mission: Over a decade in space. IEEE Journal of Selected Topics in Applied Earth Observations and Remote Sensing 6:243–256.
46. Lee CM, et al. (2015) An introduction to the NASA Hyperspectral InfraRed Imager (HyspIRI) mission and preparatory activities. Remote Sens Environ 167:6–19.
47. Thayer SS, Björkman O (1990) Leaf Xanthophyll content and composition in sun and shade determined by HPLC. Photosynth Res 23(3):331–343.
48. Papale D, et al. (2006) Towards a standardized processing of Net Ecosystem Exchange measured with eddy covariance technique: Algorithms and uncertainty estimation. Biogeosciences 3:571–583.
49. Reichstein M, et al. (2005) On the separation of net ecosystem exchange into assimilation and ecosystem respiration: Review and improved algorithm. Glob Change Biol 11:1424–1439.
50. Lyapustin A, Martonchik J, Wang Y, Laszlo I, Korkin S (2011) Multiangle implementation of atmospheric correction (MAIAC): 1. Radiative transfer basis and lookup tables. J Geophys Res Atmos 116, 10.1029/2010jd014985.

51. Lyapustin A, et al. (2011) Multiangle implementation of atmospheric correction (MAIAC): 2. Aerosol algorithm. J Geophys Res Atmos 116, 10.1029/2010jd014986.
52. Lyapustin A, Wang Y, Frey R (2008) An automatic cloud mask algorithm based on time series of MODIS measurements. J Geophys Res Atmos 113, 10.1029/2007jd00964.
53. Lyapustin A, Wang Y, Laszlo I, Korkin S (2012) Improved cloud and snow screening in MAIAC aerosol retrievals using spectral and spatial analysis. Atmos Meas Tech 5: 843–850.
54. Rahman AF, Cordova VD, Gamon JA, Schmid HP, Sims DA (2004) Potential of MODIS ocean bands for estimating CO2 flux from terrestrial vegetation: A novel approach. Geophys Res Lett 31:L10503.
55. Hollinger DY, et al. (1999) Seasonal patterns and environmental control of carbon dioxide and water vapour exchange in an ecotonal boreal forest. Glob Change Biol 5:891–902.
56. Noormets A, et al. (2010) Response of carbon fluxes to drought in a coastal plain loblolly pine forest. Glob Change Biol 16:272–287.
57. Wharton S, Falk M, Bible K, Schroeder M, Paw UKT (2012) Old-growth CO2 flux measurements reveal high sensitivity to climate anomalies across seasonal, annual and decadal time scales. Agric For Meteorol 161:1–14.

## Figure Legends

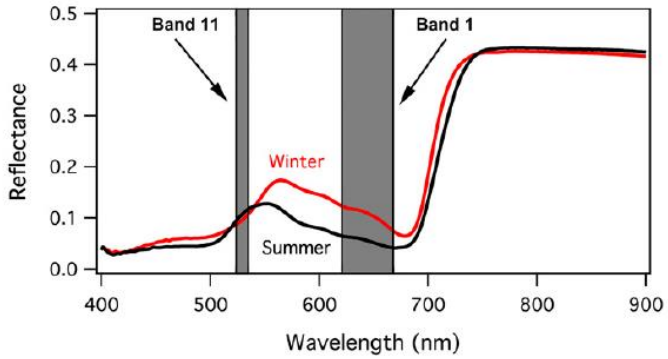


**Fig. 1** Needle reflectance spectra of *Pinus contorta* (lodgepole pine) seedlings in Edmonton, Alberta, Canada, exposed to a boreal winter (red line, March 19, 2013) and summer (black line, June 21, 2013). The positions of MODIS bands 1 and 11 are indicated in gray.

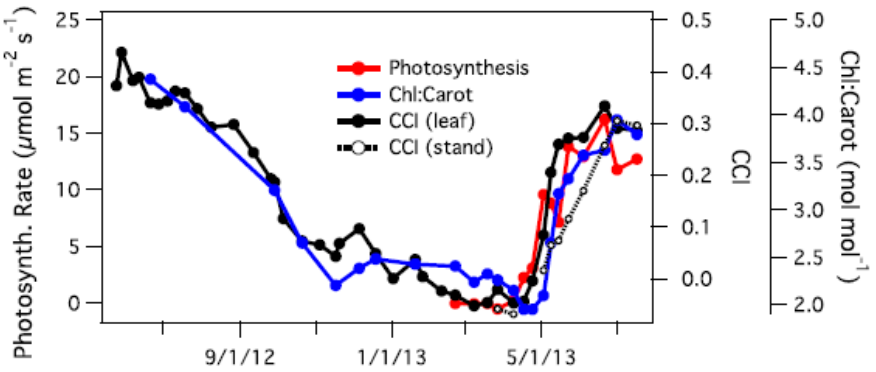


**Fig. 2** Seasonal patterns of leaf photosynthesis, leaf chlorophyll/carotenoid pigment ratios, and the CCI at the leaf (solid black line) and stand (dotted line and open circles) scales. All data were from *P. contorta* (lodgepole pine) seedlings grown in Alberta, Canada.

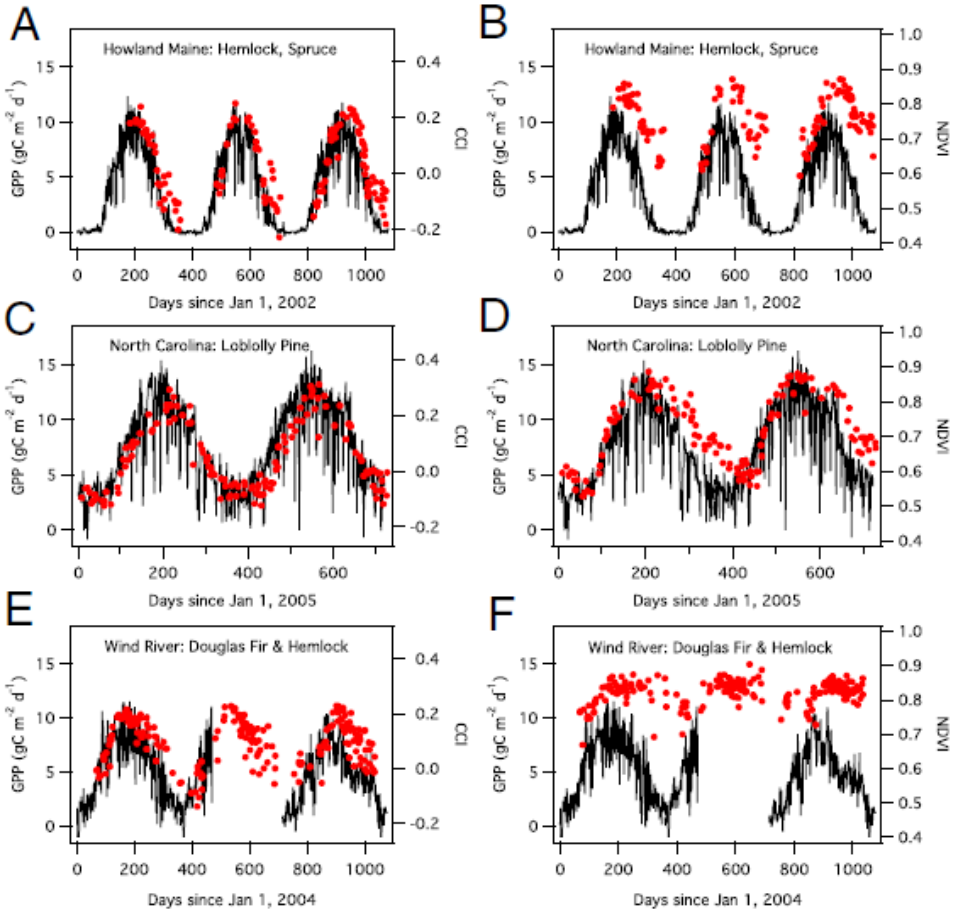


**Fig. 3** Seasonal patterns of stand photosynthesis (expressed as daily GPP, black lines), MODIS CCI (red circles; A, C, and E), and NDVI (red circles; B, D, and F) for three evergreen-dominated stands (site names and dominant vegetation are provided in individual panels).

## Suporting information

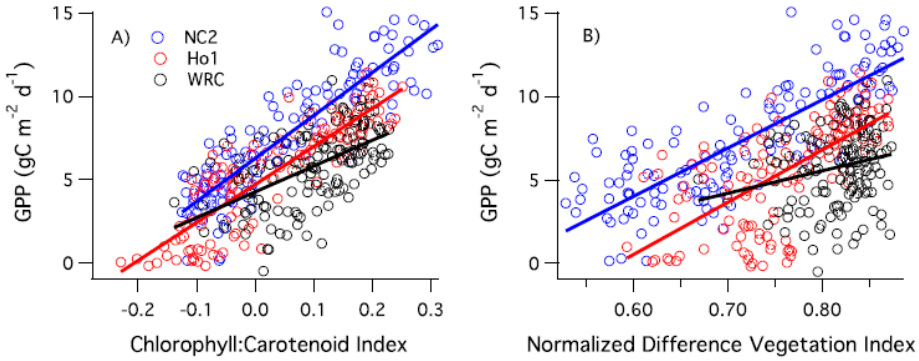


**Fig. S1.** Relationships between GPP and CCI (A) or NDVI (B) for the three sites shown in Fig. 3. Lines indicate linear fits for each site. Regression statistics are provided in Table S2. Ho1, Howland; NC2, Parker Tract, NC; WRC, Wind River.

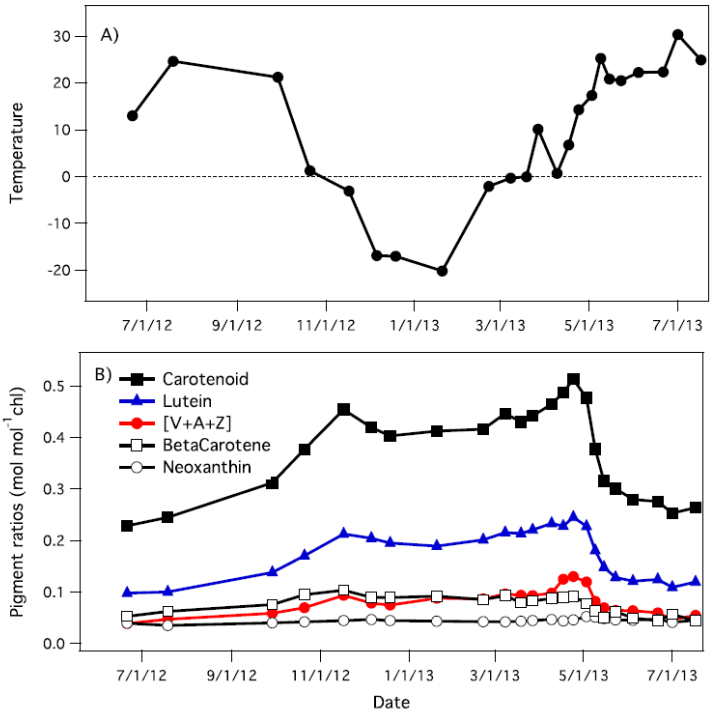


**Fig. S2.** Seasonal trends in air temperature (A) and individual carotenoid pigment pool sizes [B; relative to chlorophyll (chl)] for Pinus contorta grown in Edmonton, Alberta, Canada (Figs. 1 and 2).

**Table S1**. Key characteristics of the eddy covariance sites used in the study

| Attribute | Howland (US-Ho1) | Parker Tract (US-NC2) | Wind River (US-WRC) |
|---|---|---|---|
| Latitude | 45.2041°N | 35.8031°N | 45.8205°N |
| Longitude | 68.7402°W | 76.66791°W | 121.9519°W |
| Dominant species | Hemlock (Tsuga canadensis) and spruce (Picea rubens) | Loblolly pine (Pinus taeda) | Douglas fir (Pseudotsuga menziesii) and western hemlock (Tsuga heterophylla) |
| Contribution of deciduous species | ~11% by cover | ~35–50% by LAI; P. taeda semideciduous | Negligible (primarily understory species) |
| Biomass, $t \cdot C \cdot ha^{-1}$ | 120 ± 47 | 40-65 | 94 |
| Peak LAI, $m^2 \cdot m^{-2}$ | 4.5 | 4.0-4.3 | 8.6 |
| Age, y | 110 | 18 | 450 |
| Height, m | 20 | 16 | 56 |
| Soil type | Glacial till, fine sandy loam | Histosol | Mesic well-drained loam |
| Elevation, m | 60 | 3 | 372 |
| MAT, °C | 5.3 | 17 | 9.5 |
| MAP, mm | 1,070 | 1,320 | 5,450 |

LAI, leaf area index; MAP, mean annual precipitation; MAT, mean annual temperature. Key site characteristics are as reported in the FLUXNET2015 database (fluxnet.fluxdata.org/data/fluxnet2015-dataset/) and additional references (55–57).

**Table S2.** Regression statistics for Fig. S1

| Flux tower sites | Slope | Intercept | R2 | P |
|---|---|---|---|---|
| GPP-CCI | | | | |
| Ho1 | 22.822* | 4.7131 | 0.7646 | <2.2e-16 |
| NC2 | 25.806* | 6.2735 | 0.7765 | <2.2e-16 |
| WRC | 15.498† | 4.2715 | 0.3275 | <2.2e-16 |
| All sites | 0.681 | 4.9858 | 0.5538 | <2e-16 |
| GPP-NDVI | | | | |
| Ho1 | 31.305* | −18.254 | 0.4390 | <2.2e-16 |
| NC2 | 28.930† | −13.218 | 0.6644 | <2.2e-16 |
| WRC | 13.469‡ | −5.225 | 0.0471 | 0.00814 |
| All sites | 17.515 | 7.178 | 0.2157 | <2e-16 |

Significant differences in regression slopes (determined by analysis of covariance, $P \leq 0.05$) are indicated with different symbols.